

**$\alpha$ -transfer contribution to  ${}^9\text{Be} + {}^{13}\text{C}$  elastic and inelastic scattering**

A. Barbadoro, F. Pellegrini, G. F. Segato, and L. Taffara

*Dipartimento di Fisica dell'Università, Padova, Italy  
and Sezione di Padova, Istituto Nazionale di Fisica Nucleare, Padova, Italy*

I. Gabrielli

*Dipartimento di Fisica dell'Università, Trieste, Italy  
and Sezione di Trieste, Istituto Nazionale di Fisica Nucleare, Trieste, Italy*

M. Bruno

*Dipartimento di Fisica dell'Università, Bologna, Italy  
and Sezione di Bologna, Istituto Nazionale di Fisica Nucleare, Bologna, Italy*

(Received 6 November 1989)

Angular distributions for the  ${}^9\text{Be} + {}^{13}\text{C}$  elastic and inelastic scattering have been measured at a  ${}^9\text{Be}$  bombarding energy of 50.46 MeV over an angular range from  $10^\circ$  to  $170^\circ$  c.m. Besides the ground state of  ${}^{13}\text{C}$ , the 3.68 MeV  $J^\pi = \frac{3}{2}^-$  and the 7.55 MeV  $J^\pi = \frac{5}{2}^-$  levels are strongly populated. The enhancement of the backward cross section is a clear evidence that the process is dominated by the exchange of an  $\alpha$  particle between two identical  ${}^9\text{Be}$  cores. The experimental relative integrated cross sections are fairly well reproduced by distorted wave calculations using an  $\alpha$ -cluster form factor and the shell-model spectroscopic strengths of Kurath.

In previous studies of elastic scattering, angular distributions have been observed to be enhanced at backward angles, when both projectile and target nuclei belong to  $1p$  and  $2s-1d$  shell.<sup>1-5</sup> This effect has been found to be more pronounced when both projectile and target nuclei are integer multiples of an  $\alpha$  particle. However, the enhancement of the cross section at back angles has also

been observed when the interacting nuclei do not present such  $n\alpha$  structure, but differ by an  $\alpha$  particle as in a system like  ${}^9\text{Be} + {}^{13}\text{C}$ . This behavior has been observed by Jarczyk *et al.*<sup>3</sup> in the elastic scattering of  ${}^9\text{Be}$  on  ${}^{13}\text{C}$  at c.m. energies of 11.5 and 14.9 MeV. The high cross section in the backward direction is explained as a contribution of the  $\alpha$ -exchange process, supported also theoret-

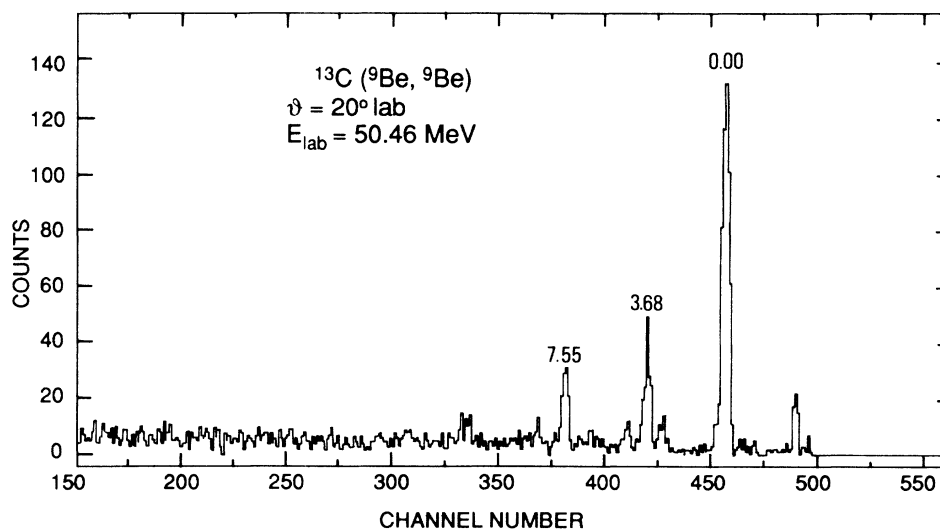


FIG. 1. Spectrum of  ${}^9\text{Be}$  ions scattered by a  ${}^{13}\text{C}$  target at an incident energy of 50.46 MeV and  $\theta_{\text{lab}} = 20^\circ$ . The peaks are labeled by the  ${}^{13}\text{C}$  excitation energy expressed in MeV.

cally by the large  $\alpha$ -cluster amplitude in  $^{13}\text{C}$  predicted by Kurath.<sup>6</sup> However, the  $\alpha$ -structure amplitudes for the  $1p$  shell nuclei computed by Kurath show large spectroscopic factors also for the negative parity excited states of  $^{13}\text{C}$ .

Therefore, if the enhancement of the backward elastic cross section has been successfully interpreted as due to an  $\alpha$ -transfer process between two identical  $^9\text{Be}$  cores, this effect should be found also in the inelastic scattering

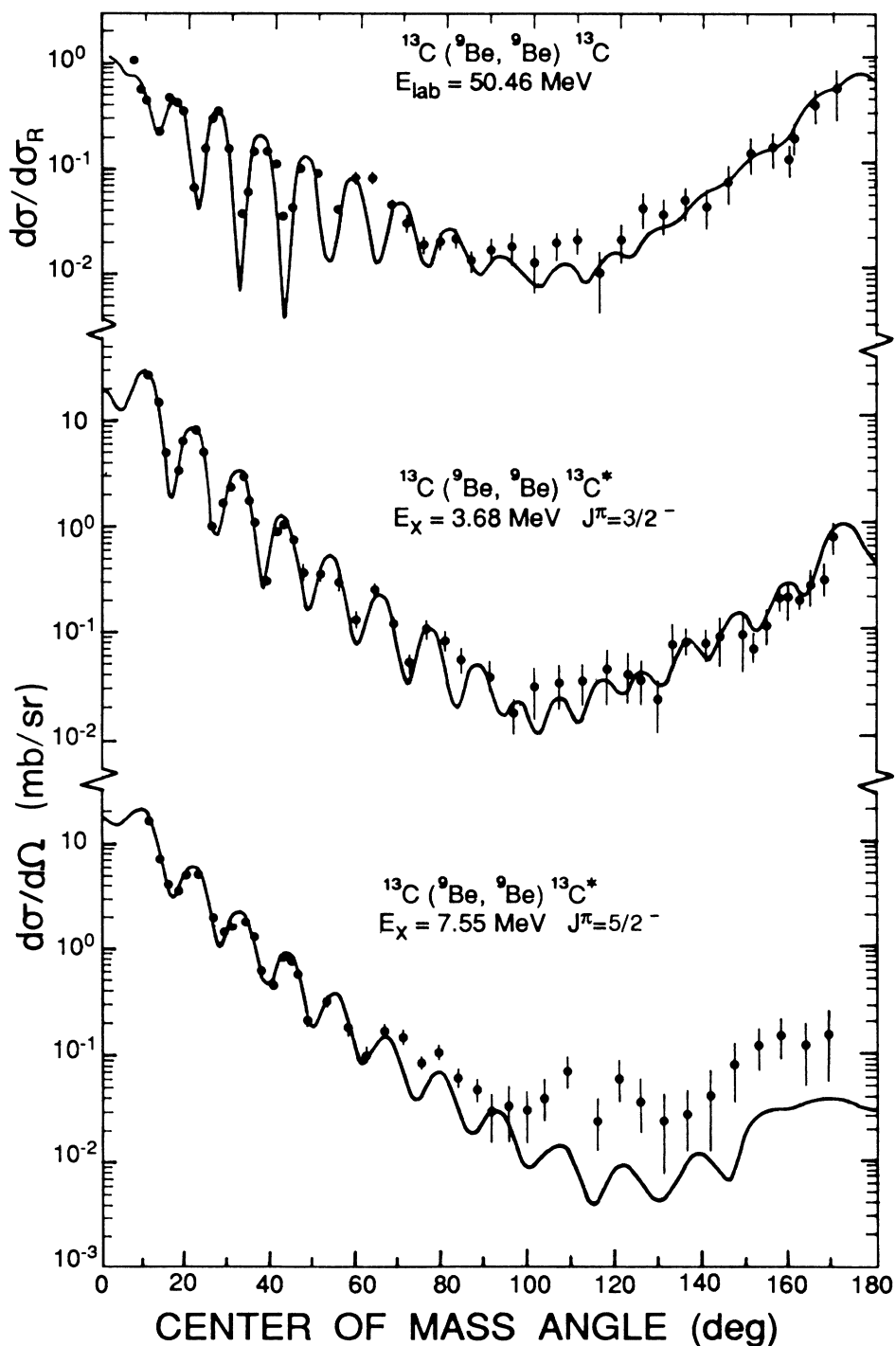


FIG. 2. Experimental angular distributions for the elastic and inelastic scattering of  $^9\text{Be}$  by  $^{13}\text{C}$  at 50.46 MeV. The error bars indicated correspond to the statistical errors only. The solid lines show the theoretical calculations resulting from the coherent and incoherent addition of the elastic (inelastic) scattering amplitude with the corresponding  $\alpha$ -transfer amplitude.

of  ${}^9\text{Be}$  ions from  ${}^{13}\text{C}$ . Animated by the intent of investigating this reaction mechanism in the inelastic process, we have undertaken at an incident energy of 50.46 MeV the present  ${}^{13}\text{C}({}^9\text{Be}, {}^9\text{Be}')$  experiment, whose results are presented in this Brief Report.

The  ${}^9\text{Be}$  beam was produced by extracting  ${}^9\text{BeO}^-$  from a sputtering ion source of the XTU Tandem of the National Laboratory of Legnaro. The  $\text{O}^-$ , as well as the outer electrons, were stripped from the  $\text{BeO}$  ions in the terminal carbon foil stripper of thickness  $5 \mu\text{g cm}^{-2}$ . The charged  ${}^9\text{Be}$  ions were further accelerated and momentum analyzed in the  $3^+$  charge state with an energy of 50.46 MeV. The target was a self-supporting  ${}^{13}\text{C}$  foil of thickness  $60 \mu\text{g cm}^{-2}$  (enriched to 96% in  ${}^{13}\text{C}$ ). The scattered ions were detected by two  $\Delta E - E$  counter telescopes angularly separated by  $5^\circ$  and mounted on a rotatable platform in a large scattering chamber of one meter diameter. Each counter telescope consisted of a 17–18  $\mu\text{m}$  Si surface-barrier  $\Delta E$  detector followed by a 400  $\mu\text{m}$  Si  $E$  counter cooled to  $-2^\circ\text{C}$ . The  $\Delta E$  and  $E$  signals were stored on magnetic tape and then sorted off line, into  $\Delta E \times E$  plots, to separate the different ion groups. In order to obtain a complete angular distribution from  $\theta_{\text{c.m.}} = 10^\circ$  up to  $170^\circ$ , the backward cross sections ( $\theta_{\text{c.m.}} > 100^\circ$ ) were determined by detecting the recoiling target nuclei at forward angles. Absolute cross sections were evaluated by reference to the elastic  ${}^{13}\text{C}({}^9\text{Be}, {}^9\text{Be}){}^{13}\text{C}$  optical model fit, with an accuracy of about  $\pm 15\%$ . A typical pulse height spectrum is shown in Fig. 1, where the energy resolution of the  ${}^9\text{Be}$  groups is of the order 250–300 keV. No  ${}^9\text{Be}$  excited states are observed since these states are particle unstable.

It is known<sup>7</sup> that the  ${}^{13}\text{C}$  spectrum presents eight levels up to an excitation energy of 8 MeV. Of these we observe only three peaks all of negative parity, that is, the ground state ( $J^\pi = \frac{1}{2}^-$ ), the 3.68 MeV ( $J^\pi = \frac{3}{2}^-$ ), and the 7.55 MeV ( $J^\pi = \frac{5}{2}^-$ ) states. These levels are populated by inelastic scattering of  ${}^9\text{Be}$ , with cross sections one order of magnitude higher than the remaining states. Such selectivity of the inelastic process proves a dominant direct reaction mechanism. As mentioned above, Kurath<sup>6</sup> has calculated the  $\alpha$ -spectroscopic amplitudes for the  $1p$  nuclei assuming a shell-model ( $1p$ )<sup>4</sup> basis. The spectroscopic strengths for the negative parity states are given in Table I. The non-negligible values of the  $\alpha$ -structure spectroscopic strengths for the negative parity states suggest that the elastic and inelastic transfer process may give an important contribution to the backward elastic

TABLE I. Spectroscopic strengths for  ${}^9\text{Be} + \alpha \rightarrow {}^{13}\text{C}$ .

$E_x$ (MeV)		$J^\pi, T$	$L_\alpha = 0$	$L_\alpha = 2$	$L_\alpha = 4$
Expt. <sup>a</sup>	Calc. <sup>b</sup>				
0	0	$\frac{1}{2}^-, \frac{1}{2}$		0.407	
3.68	3.59	$\frac{3}{2}^-, \frac{1}{2}$	0.235	0.0214	
7.55	7.40	$\frac{5}{2}^-, \frac{1}{2}$		0.0014	0.212

<sup>a</sup>From Ref. 7.

<sup>b</sup>From Ref. 6.

and inelastic cross sections. All the experimental angular distributions show indeed a pronounced backward cross section, as can be seen from Fig. 2. In this figure the theoretical curves represent the DWBA differential cross sections which take into account the elastic and inelastic  $\alpha$ -transfer process and can be written as follows:

$$\frac{d\sigma}{d\Omega} = |f_{sc}^{l_1}(\theta) - \sqrt{S_1} \sqrt{S_2(l_1)} f_{tr}^{l_1}(\pi - \theta)|^2 + \sum_{l \neq l_1} S_1 S_2(l) \sigma_l(\pi - \theta),$$

where  $f_{sc}^{l_1}(\theta)$  is the elastic or inelastic scattering amplitude which occurs with angular momentum transfer  $l_1$ , at the angle  $\theta$ , and interferes coherently with the  $f_{tr}^{l_1}(\pi - \theta)$   $\alpha$ -transfer amplitude with the same  $l_1$  transfer at the angle  $\pi - \theta$ . The remaining part is an incoherent term involving transfer momenta different from  $l_1$ .  $S_1$  and  $S_2(l)$  represent the spectroscopic factors of the  $\alpha$  cluster in the target and in the residual nucleus, respectively. For the elastic transfer, including recoil effects, we have  $l_1 = 0$  and  $l = 1, 2, 3, 4$ . For the  $\frac{3}{2}^-$  state at 3.68 MeV and for the  $\frac{5}{2}^-$  state at 7.55 MeV we have  $l_1 = 2, l = 0, 1, 2, 3, 4$  and  $l_1 = 2, l = 3, 4, 5, 6$ , respectively.

The theoretical cross sections were calculated using the code PTOLEMY (Ref. 8) for the elastic and inelastic scattering and the code LOLA (Ref. 9) for the elastic and inelastic  $\alpha$  transfer of the  ${}^{13}\text{C}({}^9\text{Be}, {}^{13}\text{C}^*){}^9\text{Be}$  reaction channel. The optical model parameters were those adopted by Jarczyk *et al.*<sup>3</sup> at lower energies and are listed in Table II. For the inelastic scattering, the Coulomb deformation parameters  $\beta_c$  have been computed by the code PTOLEMY from the  $B(E2)$  reduced transition probabilities to the ground state, evaluated from the experimental level widths<sup>7</sup> of  $(3.6 \pm 0.8) \times 10^{-3}$  eV for the 3.68 MeV state and of  $(0.115 \pm 0.007)$  eV for the 7.55 MeV level. The nuclear deformation parameters  $\beta_n$  are chosen such that the deformation lengths  $\beta_n R_n$  and  $B_c R_c$  are equal. The values  $\beta_n R_n = 1.43$  fm and  $\beta_n R_n = 1.34$  fm thus obtained for the two nuclear states of  ${}^{13}\text{C}$  are in good agreement with the value  $\beta_n R_n = 1.4$  fm derived by Mateja *et al.*<sup>10</sup> in the analysis of the inelastic  ${}^9\text{Be}$  scattering from  ${}^{12}\text{C}$  nuclei. The theoretical cross sections thus calculated reproduce very well the experimental ones in the forward direction and fairly well in the backward

TABLE II. Optical model parameters used in the DWBA calculations.

Channel	$V$ (MeV)	$W$ (MeV)	$r_0^a$ (fm)	$a$ (fm)	$r_c^b$ (fm)
${}^9\text{Be} + {}^{13}\text{C}$	-60	-32.6	1.18	0.6	1.2
${}^4\text{He} + {}^9\text{Be}$	c		1.3	0.7	

<sup>a</sup>The parameter  $r_0$  is defined by  $R = r_0(A_t^{1/3} + A_p^{1/3})$ , where  $R$  is the total radius of the potential;  $t$  and  $p$  stand for target and projectile, respectively.

<sup>b</sup>The Coulomb radius is defined as  $r_c A_t^{1/3}$ .

<sup>c</sup>Adjusted to reproduce the observed binding energy.

TABLE III. Summary of results from the  $^{13}\text{C}(^9\text{Be}, ^9\text{Be}')$  reaction.

$E_x^a$ (MeV)	$J^\pi, T^a$	Integrated cross section		Angular interval of integration (c.m.)
		Expt. (mb)	Calc. <sup>b</sup> (mb)	
0	$\frac{1}{2}^-, \frac{1}{2}$	1777±250	1659	7°–90°
		0.39±0.12	0.34	90°–170°
3.68	$\frac{3}{2}^-, \frac{1}{2}$	6.55±0.98	6.72	10°–90°
		0.38±0.11	0.40	90°–170°
7.55	$\frac{5}{2}^-, \frac{1}{2}$	4.93±0.74	5.13	10°–92°
		0.31±0.12	0.08	92°–170°

<sup>a</sup>From Ref. 7.

<sup>b</sup>The calculated cross section has been integrated in the same angular interval as the experimental one using a normalization factor for  $\alpha$ -transfer amplitude equal to  $\sqrt{528}$ . The spectroscopic factors used in the calculations are those of Table II.

direction. The results of this comparison are presented in Table III, where the only discrepancy observed is for the integrated cross section between 92° and 170° of the transition to the 7.55 MeV state. In this excitation energy region of the  $^{13}\text{C}$  nucleus, there are two levels,<sup>7</sup> the 7.49 MeV  $J^\pi = \frac{7}{2}^+$  and the  $J^\pi = \frac{3}{2}^+$  7.68 MeV, which are too close to the 7.55 MeV state to be separated by our experimental energy resolution. However, these two neighbors states have opposite parity with respect to the 7.55 MeV level, and the corresponding  $l=3$  and  $l=1$  theoretical angular distributions show a forward diffraction pattern which is out of phase with the experimental one. Thus analysis suggests that the most important contribution to the observed 7.55 MeV peak is due to the  $\frac{5}{2}^-$  state. Recently Aslanoglou *et al.*<sup>11</sup> studied the  $^9\text{Be}(^6\text{Li}, d)^{13}\text{C}$  reac-

tion to locate the  $\alpha$  strengths in  $^{13}\text{C}$ . They indeed observe a peak at 7.5 MeV whose angular distribution shows a relatively large cross section, but unfortunately no analysis has been performed to extract structure information from the experimental curve.

In conclusion, the selectivity of the  $^{13}\text{C}(^9\text{Be}, ^9\text{Be}')$  $^{13}\text{C}$  reaction is a further confirmation that the dominant primary reaction mechanism is the direct one. The enhancement of the backward cross section is well accounted with the exchange of an  $\alpha$  cluster between two identical  $^9\text{Be}$  cores. The analysis based on a cluster form factor and DWBA calculations using current shell-model wave functions and the corresponding parentage amplitudes evaluated by Kurath explains the relative yield of the observed spectrum.

<sup>1</sup>P. Braun-Munzinger and J. Barrette, Phys. Rep. **87**, 209 (1982).

<sup>2</sup>W. von Oertzen and H. G. Bohlen, Phys. Rep. **19C**, 1 (1975).

<sup>3</sup>L. Jarczyk, J. Okolowicz, A. Strzalkowski, K. Bodek, M. Hugi, J. Lang, R. Muller, and E. Ungricht, Nucl. Phys. **A316**, 139 (1979).

<sup>4</sup>Guozhu He, Chengqun Gao, and Pingzhi Ning, Phys. Rev. C **30**, 534 (1984).

<sup>5</sup>H. Takai, K. Koide, A. Bairrio Nuevo, Jr., and O. Dietzsch, Phys. Rev. C **38**, 741 (1988).

<sup>6</sup>D. Kurath, Phys. Rev. C **7**, 1390 (1973).

<sup>7</sup>F. Ajzenberg-Selove, Nucl. Phys. **A449**, 1 (1986).

<sup>8</sup>M. H. Macfarlane and S. C. Pieper, Argonne National Laboratory Report ANL 76-11, 1978.

<sup>9</sup>R. M. DeVries, Phys. Rev. C **8**, 951 (1973).

<sup>10</sup>J. F. Mateja, A. D. Frawley, P. B. Nagel, and L. A. Parks, Phys. Rev. C **20**, 176 (1979).

<sup>11</sup>X. Aslanoglou, K. W. Kemper, P. C. Farina, and D. E. Trcka, Phys. Rev. C **40**, 73 (1989).